

## Two Different Methods for Flash Drought Identification: Comparison of Their Strengths and Limitations

YI LIU,<sup>a,b</sup> YE ZHU,<sup>c,f</sup> LILIANG REN,<sup>a</sup> JASON OTKIN,<sup>e</sup> ERIC D. HUNT,<sup>d</sup> XIAOLI YANG,<sup>b</sup>  
FEI YUAN,<sup>a,b</sup> AND SHANHU JIANG<sup>b</sup>

<sup>a</sup> State Key Laboratory of Hydrology-Water Resources and Hydraulic Engineering, Hohai University, Nanjing, China

<sup>b</sup> College of Hydrology and Water Resources, Hohai University, Nanjing, China

<sup>c</sup> School of Hydrology and Water Resources, Nanjing University of Information Science and Technology, Nanjing, China

<sup>d</sup> Space Sciences and Engineering Center, Cooperative Institute for Meteorological Satellite Studies, University of Wisconsin–Madison, Madison, Wisconsin

<sup>e</sup> Atmospheric and Environmental Research, Inc., Lexington, Massachusetts

<sup>f</sup> State Key Laboratory of Hydrology-Water Resources and Hydraulic Engineering, Nanjing Hydraulic Research Institute, Nanjing, China

(Manuscript received 15 April 2019, in final form 14 February 2020)

### ABSTRACT

Flash droughts are extreme phenomena that have been identified using two different approaches. The first approach identifies these events based on unusually rapid intensification rates, whereas the second approach implicitly identifies short-term features. This latter approach classifies flash droughts into two types, namely, precipitation deficit and heat wave flash droughts (denoted as PDFD and HWFD). In this study, we evaluate these two approaches over the Yellow River basin (YRB) to determine which approach provides more accurate information about flash droughts and why. Based on the concept of intensification rate, a new quantitative flash drought identification method focused on soil moisture depletion during the onset–development phase is proposed. Its performance was evaluated by comparing the onset time and spatial dynamics of the identified flash droughts with PDFD and HWFD events identified using the second approach. The results show that the rapid-intensification approach is better able to capture the continuous evolution of a flash drought. Since the approach for identifying PDFD and HWFD events does not consider changes in soil moisture with time, it cannot ensure that the events exhibit rapid intensification, nor can it effectively capture flash droughts' onset. Evaluation of the results showed that the chosen hydrometeorological variables and corresponding thresholds, particularly that of temperature, are the main reasons for the poor performance of the PDFD and HWFD identification approach. This study promotes a deeper understanding of flash droughts that is beneficial for drought monitoring, early warning, and mitigation.

### 1. Introduction

The summer 2012 drought that occurred across the central United States is recognized as a historic flash drought event. It attracted widespread attention by the scientific community due to its tremendous impacts on agricultural production and the economy (Hoerling et al. 2014). In contrast to a traditional, more slowly evolving drought, this event intensified suddenly and caused a rapid depletion of soil moisture during a

2-month time period (Otkin et al. 2015). Trenberth et al. (2014) report that the increased heating from global warming can exacerbate drying, making the drought proceed in a more intense and quicker manner. From the perspective of its causative mechanism, such a rapid depletion of soil moisture storage often involves complicated soil moisture–atmosphere feedbacks coupled with the transition between energy-limited and water-limited conditions (Anderson et al. 2007; Otkin et al. 2013; Yuan et al. 2018). For example, enhanced evaporative demand derived from above-normal air temperatures, strong wind, or low humidity may induce a sharp decrease in soil moisture and aggravate vegetation stress (Hunt et al. 2014; Shukla et al. 2015; Hobbins et al. 2016; Ford and Labosier 2017; Liu et al. 2019). Persistent consumption of soil moisture in turn, leads to less water

Supplemental information related to this paper is available at the Journals Online website: <https://doi.org/10.1175/JHM-D-19-0088.s1>.

Corresponding author: Liliang Ren, [njrll9999@126.com](mailto:njrll9999@126.com)

DOI: 10.1175/JHM-D-19-0088.1

© 2020 American Meteorological Society. For information regarding reuse of this content and general copyright information, consult the AMS Copyright Policy ([www.ametsoc.org/PUBSReuseLicenses](http://www.ametsoc.org/PUBSReuseLicenses)).

available in the basin storage for evapotranspiration, inducing water limited conditions (Hobbins et al. 2016; Liu et al. 2017; Zhang et al. 2019).

In view of the relevant literature, there have been two different ways to identify flash droughts. One is represented by Mo and Lettenmaier (2015, 2016), which uses hydrological model simulations including soil moisture, precipitation, evapotranspiration, and temperature to identify the frequency of flash droughts in the United States. By using different combinations of thresholds for the above variables, two types of flash droughts can be classified: the precipitation deficit flash drought (PDFD) and the heat wave flash drought (HDFD). Although both types are manifested by soil moisture deficits, they originate from different physical mechanisms. The former type is initiated by negative precipitation anomalies, while the latter type is temperature driven. Several studies have employed this method to detect flash droughts in China (Yuan et al. 2015; Wang et al. 2016; Zhang et al. 2017).

Another popular method in recent literature focuses instead on the rapid intensification rate of flash drought (e.g., Ford and Labosier 2017; Otkin et al. 2018; Yuan et al. 2018; Liu et al. 2020). In their notion, the flash drought is a subset of all droughts, in that its intensification rate is unusual and should not be confused with a short-term dry spell. Otkin et al. (2018) also state that the method of flash drought identification should account for both its rapid intensification (i.e., the flash) and the actual condition of moisture limitation (i.e., the drought). Several studies have suggested that the change in soil moisture with time should be an important indicator of flash drought considering the close relationship between soil moisture and vegetation conditions (Hunt et al. 2009; Mozny et al. 2012; AghaKouchak et al. 2015; Otkin et al. 2018). For example, Ford et al. (2015) defined flash droughts as phenomena where soil moisture decreases from the 40th to 20th percentile within 20 days. Overall, such an intensification manner emphasizes the time period over which flash droughts can develop and intensify (Ford and Labosier 2017).

These two identification methods of flash droughts provide us different ways to understand this extreme phenomenon. So far, no study has made a comprehensive evaluation of these two separate approaches to illustrate which one best captures the onset time, as well as the rapid intensification process of flash drought. Based on the notion of intensification rate, here we propose a quantitative method by measuring the rate of soil moisture decline during the onset–development phase of drought to identify flash drought. The performances of the new method in monitoring flash drought events, including their onset time, and responses to variations in vegetation condition are compared with

those derived from the Mo and Lettenmaier (2016) proposed approach (i.e., PDFD and HWFD). Finally, the role of hydrometeorological variables in formulating flash droughts is investigated to interpret which method is more suitable for flash drought identification.

## 2. Study area and datasets

We used the hydrological outputs of the Variable Infiltration Capacity (VIC) model constructed over the Yellow River basin (YRB) during the period from 1961 to 2012 for flash drought analysis. The VIC model allows for the accounting of subgrid variability in soil, vegetation, precipitation, and topography for gridscale fluxes, which enables consideration of the dynamic variation in both water and energy balances (Liang et al. 1996; Wang et al. 2018). Daily meteorological forcing data required by VIC include precipitation ( $P$ ); mean, maximum, and minimum air temperature ( $T_{\text{mean}}$ ,  $T_{\text{max}}$ , and  $T_{\text{min}}$ ); wind speed; and atmospheric pressure. These data were downloaded from the China Meteorological Data Sharing Service System (<http://data.cma.gov.cn/>). Streamflow observations of five hydrological gauges with complete daily records during 1961–2012 are used for model calibration and verification. To examine the accuracy of simulated soil moisture, we also collect two sources of soil moisture products. One is from the China Agrometeorological Stations that provide 10-day relative soil moisture observations at a 50-cm depth from September 1991 to December 2012. After quality control, 57 agricultural sites with relatively long records are selected. The other is the European Space Agency (ESA) Climate Change Initiative (CCI) remote sensing soil moisture product (Dorigo et al. 2017) that has a temporal span from 1979 to 2012 with 0.25° spatial resolution. We use it to evaluate the model simulated surface soil moisture (0.05–0.1-m depth). The spatial distribution of the abovementioned meteorological, hydrological, and soil moisture sites are displayed in Fig. 1.

For model implementation, the VIC was run at a spatial resolution of 0.25° at a daily time step and was calibrated during 1961–90 and validated during 1991–2012. Figure S1 in the online supplemental material evaluates the consistency between simulated and observed streamflow series. Generally, the model can capture most of the streamflow variability with the Nash–Sutcliffe coefficients of efficiency (NSCE) varying between 0.65 and 0.94, and the absolute values of BIAS ranging from 0.3% to 10.8%. As for soil moisture verification, the VIC simulated daily values are aggregated to 10-day resolution and compared with agricultural observations. As shown in Fig. S2a, the correlation coefficients (CC) are mostly above 0.5, with higher

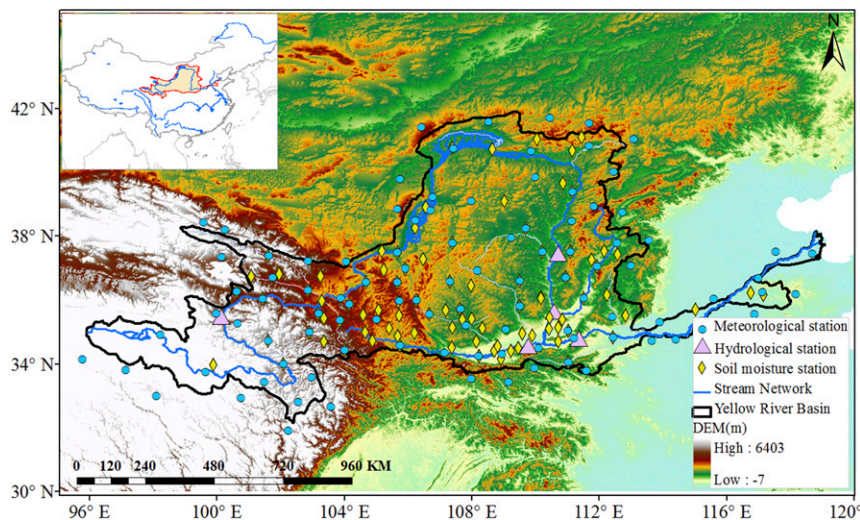


FIG. 1. Spatial distribution of national meteorological stations, soil moisture observation sites, and hydrological stations over the Yellow River basin (YRB).

CC values (up to 0.75) concentrated in the middle parts of YRB. Likewise, a good agreement is also observed between model simulated and ESA CCI soil moisture products (both are aggregated to weekly values) with CC values above 0.7 for the majority of the basin (Fig. S2b). In addition, we also compared the distribution tails of soil moisture percentiles derived from VIC simulations against those of in situ observations. The probability of detection (POD) was used to measure the consistency between VIC simulated soil moisture and in situ observations at different percentile intervals. In this study, the POD is calculated as the ratio of soil moisture percentiles at the same intervals (e.g., the soil moisture values from the VIC simulations and from the in situ observations both fall within the 40th–30th percentile) that is recorded by the VIC simulations and in situ observations simultaneously. Detailed steps for calculating the soil moisture percentiles is given in the following paragraph. As shown in Fig. S3, the POD for four intervals on average is around 0.5–0.6. Several potential factors such as the scale mismatch between model simulated soil moisture (grid scale) and in situ measurements (point scale), the accuracy of meteorological forcings (e.g., precipitation forcing) may be responsible for their disparities (Peng et al. 2017; Ford and Quiring 2019). Based on above validations of soil moisture and runoff, it is suggested that VIC model is able to depict the hydrological process in this region.

Since the rapid depletion of soil moisture is an important indicator of flash drought occurrence and also has a close relationship with vegetation status, in this study, we use soil moisture percentiles to track drought

conditions. The gridded daily soil moisture (the average values of 0–1-m soil layers) from the VIC simulations during 1961–2012 are aggregated to weekly averages. To minimize the artificial anomalies introduced by the identification method, for each grid point, percentiles are estimated separately for each calendar month. Eight candidate theoretical probability distribution functions (Table S1) are employed to fit soil moisture and other hydrometeorological variables. The optimal distribution is determined when the lowest value of root-mean-square error is achieved and also passes the Kolmogorov–Smirnov test at a 95% significance level. Likewise, other gridded outputs of VIC such as the actual evapotranspiration (AET) are also extracted to explore the dynamics of land surface and atmospheric moisture fluxes during flash drought. Particularly, several meteorological variables of VIC outputs including temperature, wind, humidity, and shortwave radiation at the surface are used to compute the potential evapotranspiration (PET) through the Penman–Monteith equation. Detailed information can be found in the official website (<https://vic.readthedocs.io/en/master/Documentation/OutputVarList/>). In addition, we also collect the Global Inventory Modeling and Mapping Studies–Normalized Difference Vegetation Index (GIMMS-NDVI) dataset to investigate the vegetation conditions, which is available semimonthly from 1982 to 2015 with a resolution of 8 km.

### 3. Methodology

#### a. Heat wave and precipitation deficit flash droughts

From the perspective of physical mechanisms, Mo and Lettenmaier (2016) defined two types of flash droughts,

that is, heat wave and precipitation deficit flash droughts (denoted as HWFD and PDFD). Although both types are manifested by soil moisture deficits (below 40% percentile), they substantially reflect different propagation chains of moisture and energy fluxes. For HWFD, high temperature is the main driver, which further leads toward increases in AET. Meanwhile, negative  $P$  anomalies before drought onset are also necessary conditions to bring down soil moisture anomalies. In a different manner, the PDFD is precipitation driven. The lack of precipitation prior to drought onset is responsible for the reduction in soil moisture and AET, which in turn leads to high temperatures. Mo and Lettenmaier (2015, 2016) tested different scenarios of multivariable based thresholds and recommended the following criteria for identifying flash droughts:

$$\text{HWFD: } T_{\text{anomaly}} > \sigma; \text{ AET}_{\text{anomaly}} > 0; P_{\text{anomaly}} < 0; \\ \text{SM} < 40\text{th percentile}, \quad (1)$$

$$\text{PDFD: } P < 40\text{th percentile}; \text{ AET}_{\text{anomaly}} < 0; \\ T_{\text{anomaly}} > \sigma; \text{ SM} < 40\text{th percentile} \quad (2)$$

where  $T_{\text{anomaly}}$ ,  $P_{\text{anomaly}}$ , and  $\text{AET}_{\text{anomaly}}$  represent the anomaly of weekly air temperature, precipitation, and AET, respectively;  $\sigma$  represents the standard deviation of the  $T_{\text{anomaly}}$  series. For each grid, the HWFD and PDFD events are identified when all corresponding requirements are satisfied.

### b. Intensification rate–based flash droughts

Following the suggestion of Otkin et al. (2018), here we propose a quantitative method to identify flash droughts by focusing on the rate of intensification (RI). Unlike a more traditional, slowly evolving drought, flash drought is characterized by the rapid depletion of soil moisture resulting from a period of abnormally warm and dry weather conditions. In this sense, flash drought can be viewed as a subset of all droughts (e.g., meteorological, agricultural, and hydrological droughts), and which is most likely to occur in the onset–development phase of the drought event. As shown in Fig. 2a, suppose  $t_1$  is the onset time that the soil layer is experiencing the “abnormally dry” conditions and has the potential to precede a drought, and the time node  $t_5$  represents the stationary point that moisture deficits suffer abrupt changes from rapid decline to smooth fluctuations (e.g.,  $t_6$ – $t_{15}$  in Fig. 2a) or even present an increased pattern (e.g.,  $t_{15}$ – $t_{18}$  in Fig. 2a). In other words, the stationary point can be viewed as the termination of rapid soil moisture reduction, which may emerge at or before the peak of drought intensity. With this in mind, the identification of flash droughts is further generalized as two questions: how to extract the

onset–development phase (i.e., the time period from  $t_1$ – $t_5$ ) of droughts, and how fast should the intensification be to be recognized a flash drought?

In this study, we use weekly soil moisture percentiles to depict the drought process (Fig. 2b). Specifically, drought events are extracted when the soil moisture falls below a predetermined value. Similar to previous studies, the threshold adopted here is twofold: 1) soil moisture is less than the 40th percentile, and 2) the peak drought intensity must fall below the 20th percentile (Ford and Labosier 2017; Otkin et al. 2018). The onset time (i.e.,  $t_1$  in Fig. 2a) of a flash drought event, therefore, is defined as the first week when the soil moisture falls below the 40% percentile. As for the stationary point (i.e.,  $t_5$  in Fig. 2a), a univariate polynomial function is employed to determine its location along the horizontal axis (viz., the date in Fig. 2a). Figure 3 presents four typical examples of the attenuation process of soil moisture percentiles under drought. All points between the onset time and peak of intensity are used when searching for the fitting equation. When a linear regression function is employed, the peak of drought intensity is chosen as the stationary point (Fig. 3a). With respect to the nonlinear case, we increase the order of the polynomial in sequence (e.g., linear polynomials, quadratic, cubic, ...,  $n$ th-order polynomial) until a minimum value of 0.95 for the deterministic coefficient  $R^2$  of fitting polynomial is attained (Figs. 3b–d). In calculus, the stationary point (i.e.,  $t_5$  in Fig. 2a) can be located when the first derivative of the constructed polynomial equals zero (i.e.,  $\partial Y/\partial X = 0$ ). In other words, the polynomial function is only used to judge when the flash drought event terminates but would not participate in estimating the magnitude of the flash drought intensification. With the extracted stationary point, the mean intensification rate ( $\text{RI}_{\text{mean}}$ ) of a drought event during its onset–development phase can be calculated as

$$\text{RI}_{\text{mean}} = \frac{1}{n} \sum_{i=1}^n \left[ \frac{\text{SM}(t_{i+1}) - \text{SM}(t_i)}{t_{i+1} - t_i} \right], \quad t_1 \leq t_i \leq t_n, \quad (3)$$

where  $t_1$  denotes the onset time, and  $t_n$  represents the stationary point. A similar concept of  $\text{RI}_{\text{mean}}$  is also employed in several previous studies. For instance, Ford and Labosier (2017) recommended that the soil moisture content dropping from the 40th percentile to below the 20th percentile in no less than 4 pentads (equivalent to a  $\text{RI}_{\text{mean}}$  value of 6.5 percentile per week) could be recognized as flash droughts. Given the similar climatic characteristics between the YRB and their research area (i.e., Oklahoma, United States), in this study we use the same metric to identify flash droughts, which puts more emphasis on the overall declining rate of soil moisture during the whole onset–development period. However,

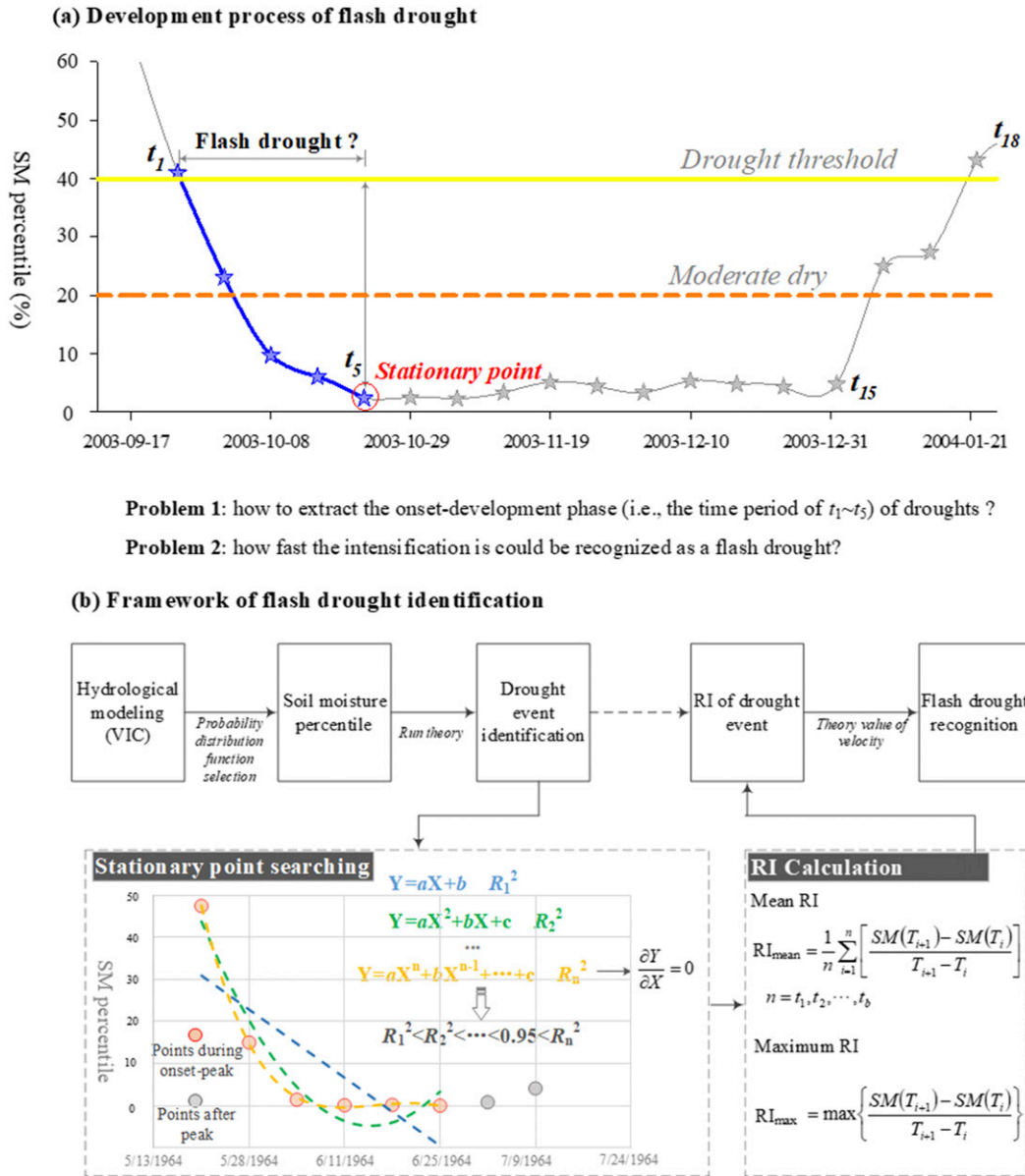


FIG. 2. (a) Schematic overview of the evolution process of flash drought indicated by soil moisture percentile;  $t_1$  represents the onset time;  $t_5$  denotes the stationary point where rapid depletion of soil moisture ends; the period from  $t_6$  to  $t_{18}$  represents the recovery stage where soil moisture increases gradually then returns to the normal condition. (b) Generalized flowchart of identifying flash drought based on intensification rate. The left dashed rectangle shows how find the stationary point with the polynomial fitting method. The left rectangle gives the formulas for calculating the rate of intensification.

in reality, there may exist some exceptional cases that their  $RI_{\text{mean}}$  is lower than the predetermined value (i.e., 6.5 percentile per week) but have rather high instantaneous  $RI_i$  values at a certain moment. We determined that such cases should also be considered flash droughts. On these grounds, the instantaneous maximum intensification rate ( $RI_{\text{max}}$ ) during the onset–development phase is introduced:

$$RI_{\text{max}} = \max \left[ \frac{SM(t_{i+1}) - SM(t_i)}{t_{i+1} - t_i} \right], \quad t_1 \leq t_i \leq t_n. \quad (4)$$

A flash drought is recognized when either the condition of  $RI_{\text{mean}}$  or  $RI_{\text{max}}$  is met over a sufficiently long enough period of time. For  $RI_{\text{max}}$  selection, we make a sensitivity test on the frequency of occurrence (FOC);

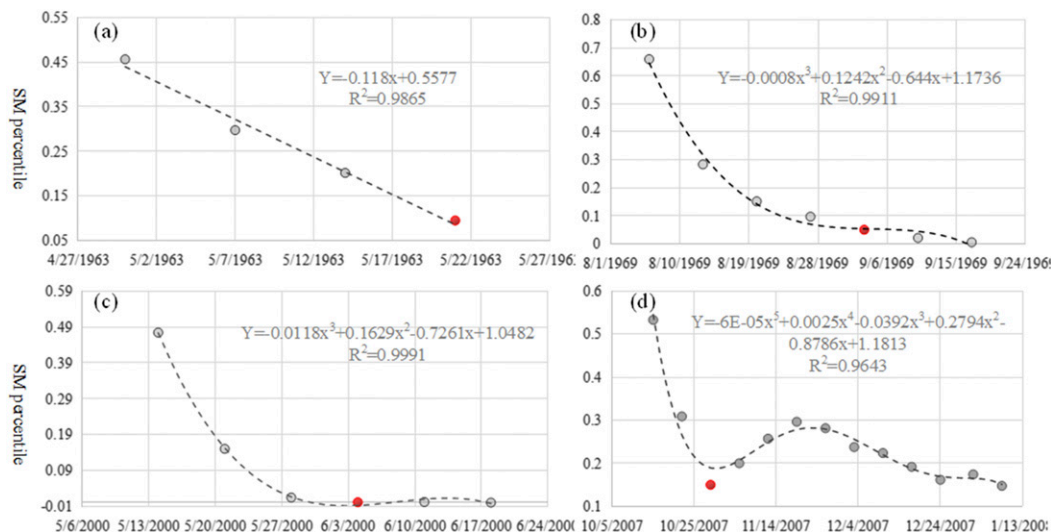


FIG. 3. Four typical examples of the attenuation process of soil moisture percentile (from the onset time to the peak of drought intensity) under drought. Based on the trajectories of soil moisture percentile, we use different order polynomials to fit these samples, and the red circles can be derived as the stationary point (when the partial derivative of the fitted polynomial equation is 0) of the established polynomial. When a linear regression function is employed, the peak of drought intensity is the stationary point.

the percent of weeks under flash drought) of flash droughts to varied  $RI_{\text{mean}}$  and  $RI_{\text{max}}$ . As shown in Fig. 4, smaller values of  $RI_{\text{mean}}$  and  $RI_{\text{max}}$  would correspond to higher FOC, and vice versa. When  $RI_{\text{mean}}$  is set to 6.5 percentile per week, the FOC of flash droughts mainly varies between 4% and 12% depending on different  $RI_{\text{max}}$  values. In this study, a value of 10 percentiles per week is selected for  $RI_{\text{max}}$ , with corresponding FOC approximate to 10%. This frequency is generally in accordance with Mo and Lettenmaier (2015, 2016), which ensures the significance of comparison between the two different methods. The flash drought based on the modified rate of intensification approach (i.e.,  $RI_{\text{mean}} > 6.5$  percentile per week or  $RI_{\text{max}} > 10$  percentile per week) is denoted as RIFD.

In the following section, we will compare RIFD against HWFD and PDFD, and explore the underlying reasons for their differences.

## 4. Results and discussion

### a. Comparison of identified flash drought events

Based on the approaches described above, a cross comparison of flash droughts identified from two different methods is conducted. As a subset of drought, one basic feature of flash droughts is that the event should fall into drought during the evolution process. Although both methods employed the 40th percentile of soil moisture to identify the onset of flash drought, it actually only represents a drier condition than normal but not

drought. For soil moisture drought, conditions less than the 30th percentile are commonly recognized as mildly dry, and less than the 20th percentile for moderate drought (Ford et al. 2015). In this sense, the RIFD method meets the condition of moisture limitation due to its secondary threshold, namely the soil moisture should be lower than the 20th percentile for at least one week. In contrast, the HWFD and PDFD make no such restrictions on soil moisture, which may lead to

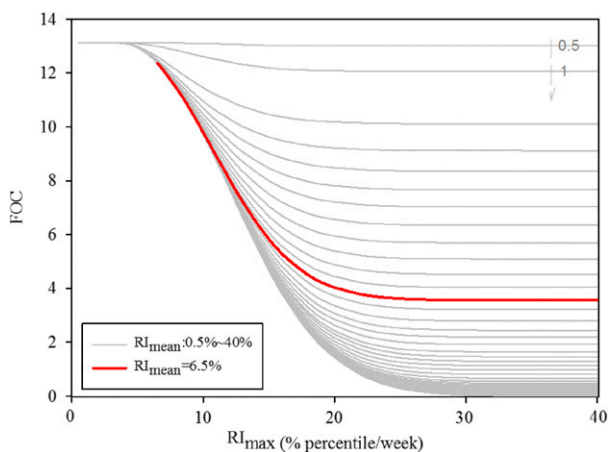


FIG. 4. Sensitivity analysis on the frequency of occurrence (FOC) of flash droughts to varied  $RI_{\text{mean}}$  and  $RI_{\text{max}}$ . The gray solid lines show the relationship between  $RI_{\text{max}}$  and FOC under different values of  $RI_{\text{mean}}$  (increasing gradually from 0.5 to 40 percentile per week). Likewise, the red solid line gives the case when  $RI_{\text{mean}} = 6.5$  percentile per week.

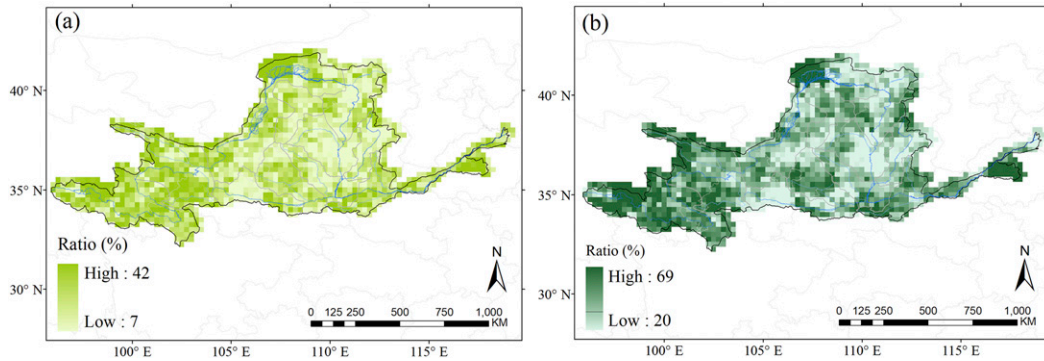


FIG. 5. (a) The ratio of nondrought events (viz., for an identified flash drought event, the soil moisture values at each week are all higher than the 30th percentile) to all events identified by HWFD and PDFD. (b) As in (a), but for the ratio of nonmoderate drought events (higher than the 20th percentile) to all events.

misjudgment of the results. Given this, we further extracted the nondrought events (i.e., for an event, the soil moisture is higher than the 30th percentile during each week) and nonmoderate drought events (higher than the 20th percentile) from HWFD and PDFD. As shown in Fig. 5, approximately 7%–40% of the identified flash drought events by HWFD and PDFD were nondrought (i.e., soil moisture of such events are above the 30th percentile), and 20%–69% were nonmoderate drought (i.e., soil moisture of such events are above the 20th percentile). This suggests that the HWFD and PDFD method could not guarantee that all of the identified events fall into drought. From the perspective of drought characteristic, these improperly recognized flash droughts were mostly minor events with their duration no more than 4 weeks. In the following section, we will remove these minor events from further analysis.

Another important feature of flash drought lies in the unusually rapid intensification rate of soil moisture deficit (i.e., the “flash” characteristic). Figure 6 presents the variation of soil moisture percentile for major flash drought events (events with duration less than 4 weeks were excluded) of all grids in the study region. For RIFD, most of the events present sharp declines in soil moisture with the moisture condition changing from normal status (above the 40th percentile) to moderate drought (below the 20th percentile) within two weeks (Fig. 6a). As for HWFD and PDFD, it on average takes five weeks (from  $T_{t-1}$  to  $T_{t+4}$ ) for soil moisture to decrease from the 18th to 10th percentile (the dark solid line in Fig. 6b). According to Eqs. (3) and (4), this depletion rate of soil moisture is equivalent to  $-1.6$  percentile per week, which is far slower than the intensification rate of RIFD (i.e.,  $-6.5$  percentile per week). Figure 7 further shows the frequency distributions of the mean and maximum rate of intensification for HWFD and PDFD

events. Generally, the HWFD statistics presented a quasi-normal distribution where approximately 80% of the events had a negative value of  $RI_{\text{mean}}$  (i.e.,  $RI_{\text{mean}} < 0$ ), but only 24% of the events identified fell below the threshold of RIFD (i.e.,  $RI_{\text{mean}} < -6.5$ ). In addition, a small percentage amount (approximately 20%) of  $RI_{\text{mean}}$  still presented positive values (i.e.,  $RI_{\text{mean}} > 0$ ), implying that the HWFD events defined by Mo and Lettenmaier (2015) may have occurred in the recovery phase where an incremental increase in soil moisture emerges. Similar patterns were also observed in  $RI_{\text{max}}$  of HWFD, and  $RI_{\text{mean}}$  and  $RI_{\text{max}}$  of PDFD (Fig. 7b). These phenomena are not limited to our study domain (YRB). Wang and Yuan (2018) found that 10%–18% of HWFD and PDFD happened in the recovery phase of seasonal droughts over China.

The above comparison demonstrates the sensitivity of results to the method of flash drought identification. Since the way for extracting HWFD and PDFD (Mo and Lettenmaier 2015; 2016) only focuses on the threshold of related variables (e.g., precipitation and temperature) and neglects changes in soil moisture with time (Otkin et al. 2018), the method can hardly ensure that the identified events satisfy the moisture limitation (i.e., the drought) and have the characteristic of rapid intensification (i.e., the flash).

#### b. Frequency of flash droughts

Figure 8 shows the spatial distribution of the FOC (the ratio of weeks under flash drought) indicated by these two methods. For RIFD, the FOC on average varied between 3% and 10%, with high occurrence of flash drought concentrated in the northwestern, southeastern, and southern of source regions (Fig. 8a). As for the two types of flash drought defined by Mo and Lettenmaier (2015, 2016), different patterns of FOC were observed both in the magnitude and spatial distributions.

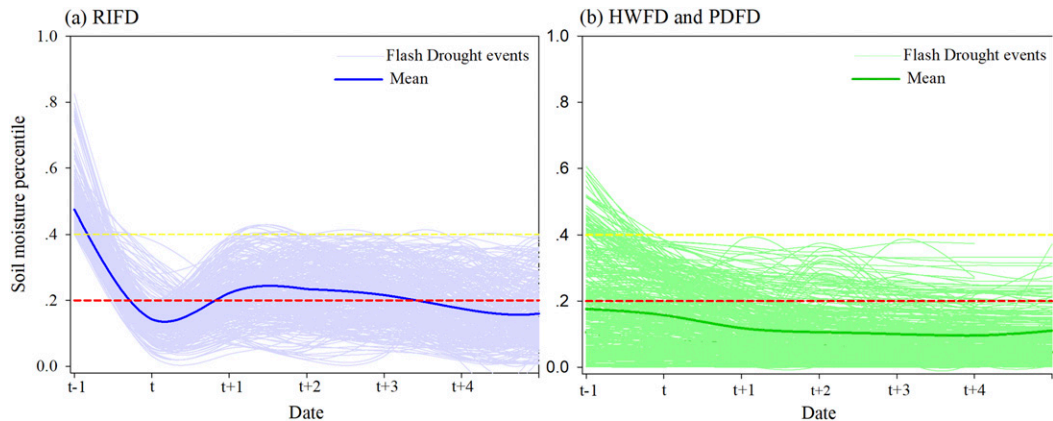


FIG. 6. Variation of soil moisture percentile for major flash drought events (light colored lines; excludes drought duration less than 4 weeks) of all grids in the study region identified by (a) RIFD and (b) HWFD and PDFD. The dark color line represents the ensemble-mean of all flash drought events. The  $t$  represents the time when the flash droughts occur. The  $t - 2$  and  $t - 1$  denote the 1 week and 2 weeks prior to  $t$ , while  $t + 1$ – $t + 4$  represent the lagged 1–4 weeks of  $t$ , respectively.

Specifically, the FOC of HWFD on average was less than 3%, with high values located in the southern region. With respect to the PDFD type, the magnitude of FOC increased to 4%–6%, and spatially the source region experienced a lower flash drought frequency. Taking HWFD and PDFD as a whole (i.e., events of HWFD and PDFD were merged into a new sample for calculating FOC), the FOC ranged between 5% and 10%, and presented an increased pattern from northwest to southeast (Fig. 8d). This suggests that different ways for identifying flash droughts would affect drought frequency to some extent. In addition, Wang and Yuan (2018) also analyzed flash drought frequency in China based on the method of Mo and Lettenmaier (2015, 2016), and suggested a similar spatial distribution of

HWFD and PDFD with our results, but the values of FOC were generally higher. The different source of soil moisture dataset (global reanalysis products were employed in their study) might be one possible reason. The time period of interest may be another possible reason (Liu et al. 2016) because their study mainly reflects the overall dry status during 1979–2010, which has a different climate condition from 1961 to 2012.

### c. Behavior in tracking flash drought

The 1991 flash drought event is selected to explore how the two methods behave in monitoring the spatial evolution of soil moisture. As shown in Fig. 9a, the drought event indicated by soil moisture percentile experienced continuous reduction starting in June 1991

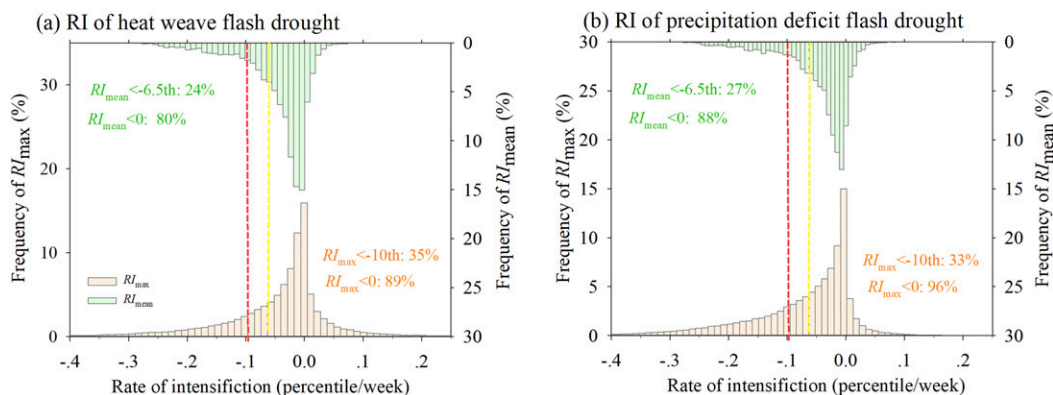


FIG. 7. (a) The frequency distributions of the mean (the green bar) and maximum (the orange bar) rate of soil moisture decline for all heat wave flash droughts (HWFD) during 1961–2012 over the entire domain. (b) As in (a), but for the  $P$ -deficit flash droughts (PDFD). The dotted red and yellow lines in (a) and (b) show the two metrics of  $RI_{max}$  (–10 percentile per week) and  $RI_{mean}$  (–6.5 percentile per week), respectively, for identifying flash droughts.

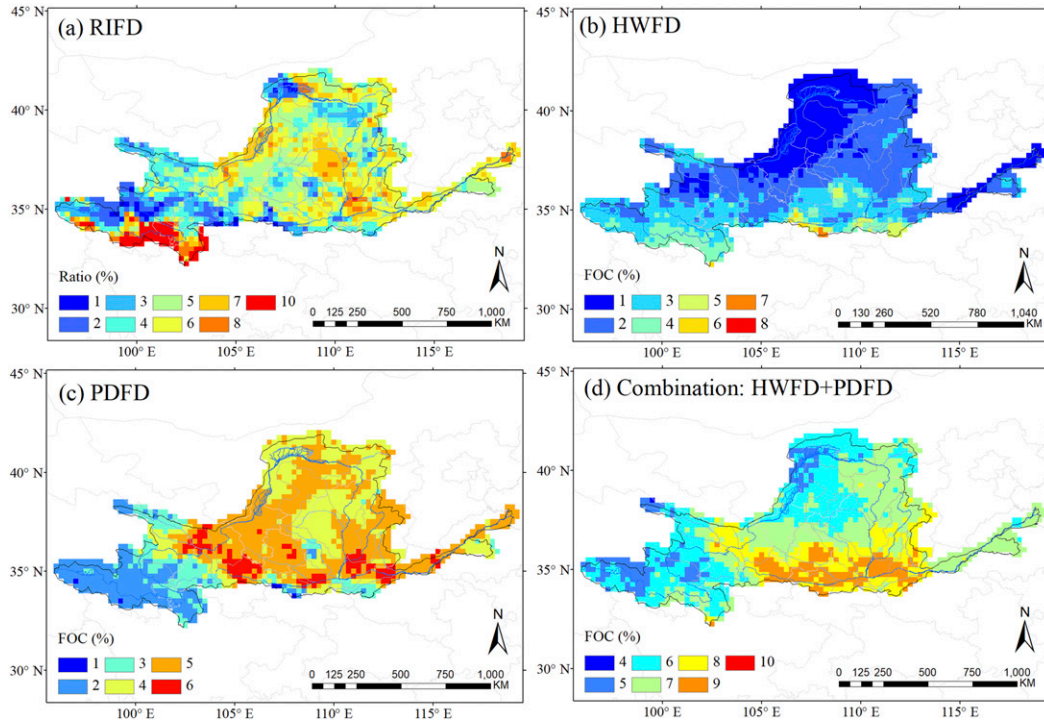


FIG. 8. Spatial distribution of the FOC for flash droughts indicated by (a) RIFD, (b) HWFD, (c) PDFD, and (d) sum of HWFD and PDFD (i.e., events of HWFD and PDFD were merged into a new sample for calculating FOC).

and sustains a rather low value (approximately one-third of the basin area is below the 10th percentile) until the next year. During this process, the period from June to July exhibits a rapid rate of intensification during which the soil moisture percentile sharply decreases from above the 40th percentile to below the 20th percentile over four weeks. Meanwhile, a spatial migration pattern is apparent for the dry condition. As shown in Fig. 9b, the drought center generally experiences a western–eastern–northern shifting mode, with the vegetation types of grassland, cropland, and shrubland suffering in sequence. This spatial variation of vegetation condition is also reflected by the 15-day NDVI anomalies (Fig. 9c). In the following section, we pay special attention to the abilities of each methods to depict the drought migration pattern, as well as in capturing the instantaneous variation of soil moisture.

The initial drought patches, as indicated by the soil moisture percentile, emerge in the source region of YRB on 11 June (Fig. 9d). This dry signal is also captured by  $RI_{\text{mean}}$  and  $RI_{\text{max}}$  but missed by HWFD and PDFD. In the following week (18 June), the latter method again fails to display dry conditions. According to the NDVI anomalies (Fig. 9c), some parts of the source region exhibited negative values on 21 June, implying that the vegetation health starts to decline, which also signifies the onset of this flash drought event. In such cases, we consider that the ways of defining

HWFD and PDFD are less competent to provide early warning for flash drought.

In addition, the HWFD and PDFD may separate a continuous process of flash drought into several independent events and can hardly characterize the spatio-temporal variation of moisture dynamics. For example, both HWFD and PDFD indicate droughts in the source region on 25 June, which is in agreement with the pattern of soil moisture percentile. But in the following week (2 July), the lower values of soil moisture move farther eastward; HWFD and PDFD by contrast, indicate nondrought and fail to capture the spatial migration of this event.

#### d. Roles of hydrometeorological variables in formulating flash droughts

A potential reason for the unsatisfying performance of the HWFD and PDFD methods could be attributed to the thresholds of hydrometeorological variables that they employ. As mentioned in section 3a, except for soil moisture, their method involves:  $P$  anomaly  $< 0$  or  $P$  percentile  $< 40\%$ ;  $T_{\text{mean}}$  anomaly  $> 1$  standard deviation; AET anomaly  $> 0$  for HWFD, and AET anomaly  $< 0$  for PDFD. In recent papers, other variables such as PET and maximum air temperature ( $T_{\text{max}}$ ) are also recommended as indicators (Hobbins et al. 2016; Zhang et al. 2017; Otkin et al. 2018). Given this,

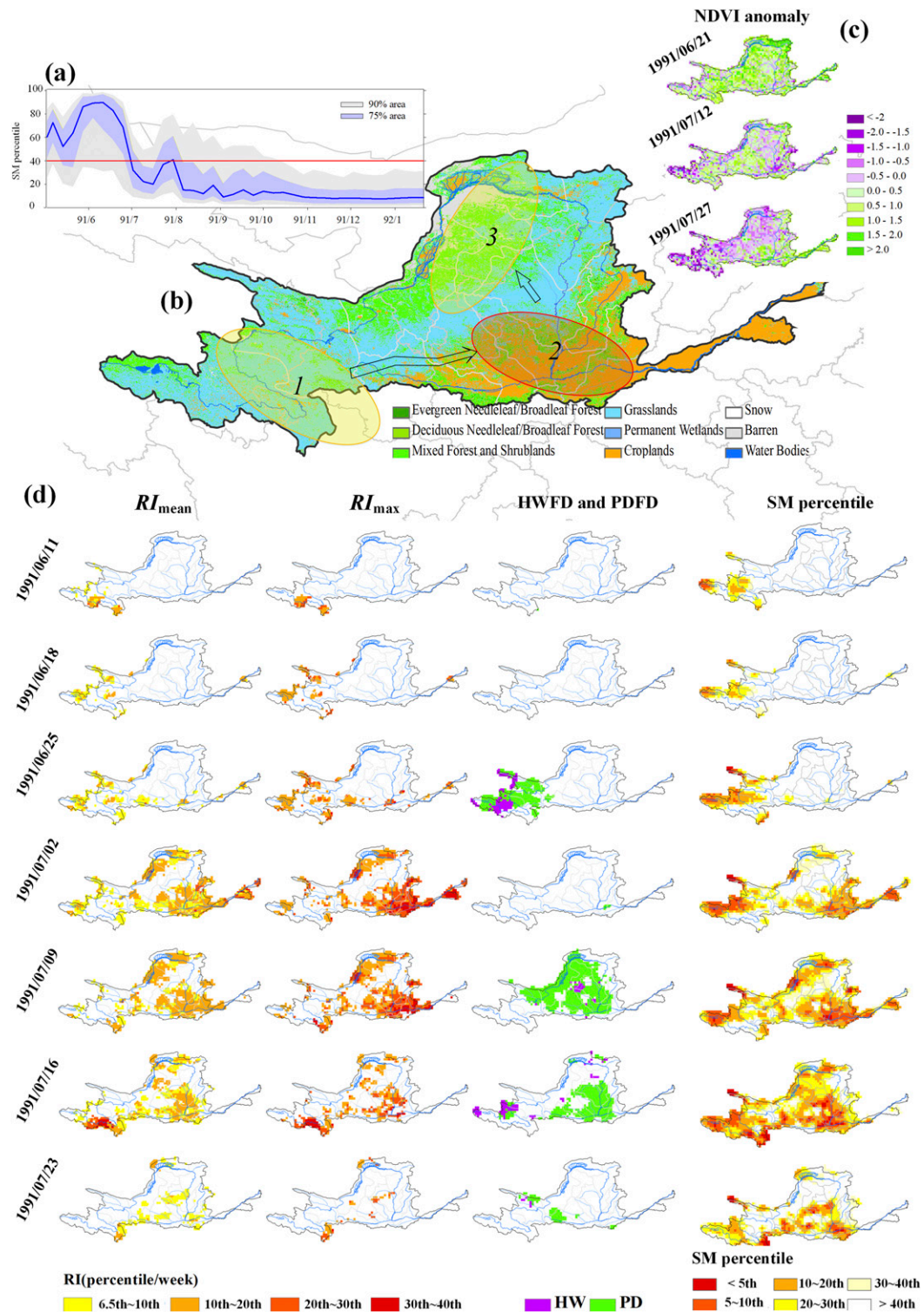


FIG. 9. (a) Time series of weekly soil moisture percentile in 1991. The gray and blue shadows denote the 75th–90th percentile range of soil moisture values over YRB. (b) The three circles with numbers in the middle indicate the moving path of the drought center during June–July in 1991. (c) Spatial evolution of NDVI anomalies (dimensionless; minus the mean then divided by the standard deviation) in June and July 1991. (d) Spatial evolution of the mean and maximum intensification rate of soil moisture, two types of flash droughts defined by Mo and Lettenmaier (2015, 2016), and soil moisture percentile in June and July 1991.

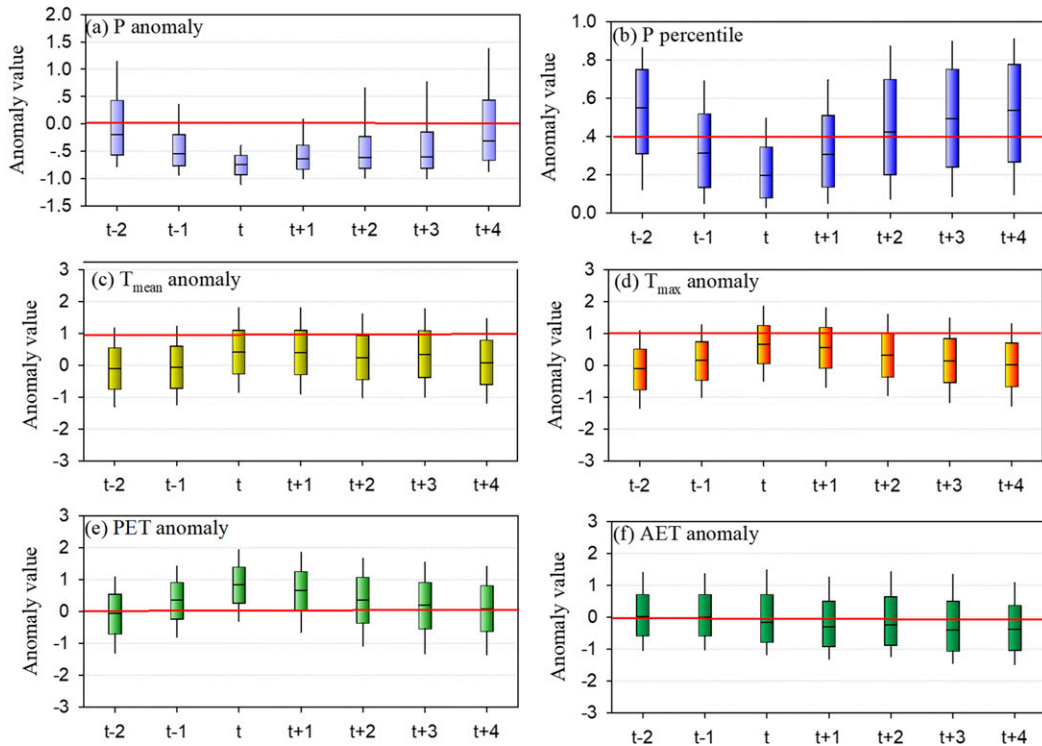


FIG. 10. Boxplots of the anomaly values of hydrometeorological variables in adjacent weeks of the onset of all flash drought events during 1961–2012 extracted from all grid cells over YRB. The red solid lines in each panel indicate the thresholds given by Mo and Lettenmaier (2015, 2016). The  $t$  represents the time node when the flash droughts occur. The  $t - 2$  and  $t - 1$  denote the 1 week and 2 weeks prior to  $t$ , while  $t + 1$ – $t + 4$  represent the delayed 1–4 weeks of  $t$ , respectively. The anomalies of all meteorological variables were dimensionless and derived by subtracting the climatological (1961–2012) mean then dividing by the standard deviation of that calendar week.

an investigation on the anomalies (percentile) of related hydrometeorological variables is conducted.

Figure 10 shows the hydrometeorological anomaly values in adjacent weeks of the onset of all flash drought events during 1961–2012 extracted from all grid cells over YRB. The anomalies of all meteorological variables were derived by subtracting the climatological (1961–2012) mean then divided by the standard deviation of that calendar week. As shown in Fig. 10a, the  $P$  anomalies are all negative and below 0.5 standard deviation at the week  $t$  (i.e., the first week when flash drought occurs), which is consistent with the condition (i.e.,  $P$  anomaly  $< 0$ ) set in Mo and Lettenmaier (2015, 2016). Moreover, for 1 week prior to  $t$  (i.e.,  $t - 1$ ), more than 75% of flash drought events are under negative  $P$  anomalies, suggesting that this threshold can provide some utility for flash drought early warning. The case of the 40th  $P$  percentile, in contrast, presents considerable spatial variability and does not work well for all regions of YRB. In Fig. 10b, it can be seen that there exist some cases when precipitation is above the 40th percentile and flash drought occurred. In fact, this phenomenon is not limited to the  $P$  percentile; similar patterns are also

observed in  $T_{\text{mean}}$  and  $T_{\text{max}}$  but in a more significant way. As shown in Figs. 10c and 10d, for the majority of flash drought events in the YRB, corresponding air temperature values rarely exceed one standard deviation. This means substantial flash drought events would be excluded by this truncated level. To verify this conjecture, the spatial variation of these thresholds during June–July in 1991 is investigated (Fig. 11). Obviously, the  $T_{\text{mean}}$  anomaly is the main factor for the poor performance of the HWFD and PDFD. In contrast, the AET anomaly is generally above normal in the early period of flash drought (11 June in Fig. 11) and exhibits negative values when the conditions become water limited (the  $P$  anomaly is significantly negative and the PET anomaly is positive). This indicates that AET may not be a good indicator of flash drought. It plays a minimal role in judging whether or not flash drought occurs; however, it does have some implications for understanding the physical mechanisms of heat wave and precipitation deficit flash droughts (Figs. 10f and 11). A similar phenomenon was also found in the central United States, where the anomalies of evaporation do not appear to be stronger during the flash drought

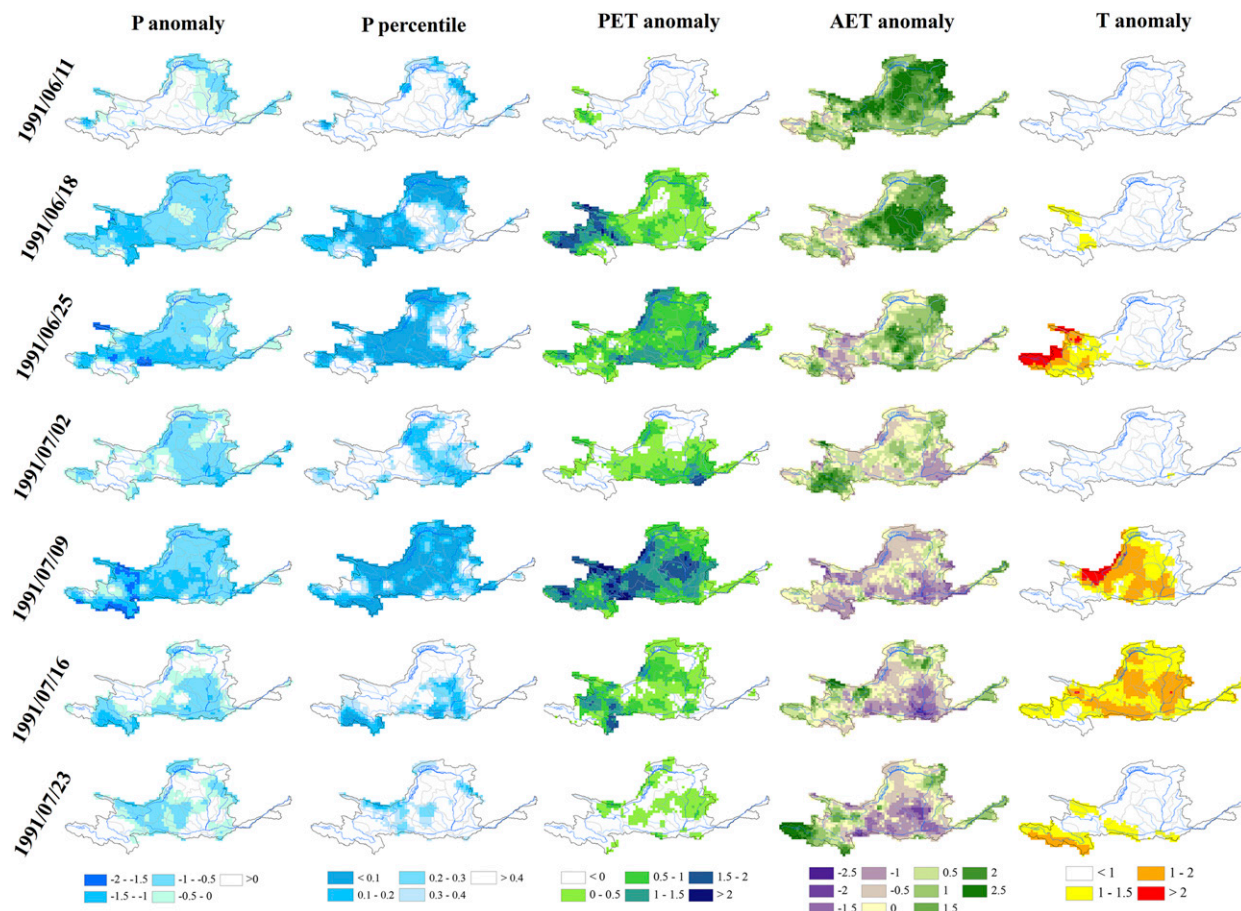


FIG. 11. Spatial anomalies of related meteorological variables for the 1991 flash drought.

onset (Koster et al. 2019). From the perspective of atmospheric evaporative demand, PET integrates the effects of wind, humidity, temperature, and solar radiation, which can be viewed as a more comprehensive indicator of how much moisture is consumed. As shown in Fig. 10e, more than half of the PET anomalies exhibit positively biased patterns at week  $t - 1$ , then the evaporative demand quickly expands and reaches the peak at the onset of flash drought. In other words, PET anomalies can vary synchronously with the soil moisture dynamics during the flash drought process and could be viewed as a driver in the changes of soil moisture (Hobbins et al. 2016; Otkin et al. 2018).

In general, the unsatisfying performance of HWFD and PDFD can be attributed to two aspects, that is, the variable selection and corresponding thresholds. The case study in YRB suggests the overly rigid threshold of temperature (i.e.,  $T_{\text{mean}}$  anomaly  $> 1$  standard deviation) may lead to some omission in capturing the onset of the event. Some trials by lowering the threshold of the temperature anomaly (e.g., relaxing from one standard deviation to a half standard deviation or other values

according to the climate conditions and soil moisture dynamics of the study region) can be made in future studies to improve the performance of HWFD and PDFD. In contrast, PET exhibits the potential of being a precursor signal for indicating drought and can be employed as an alternative in future studies. In addition, since more attention is given to the occurrences of flash drought in determining the thresholds of related variables, the approach proposed by Mo and Lettenmaier (2016) can hardly guarantee the identified events all have the rapid intensification characteristic. An improved flash drought identification result would be expected by introducing the intensification rate in their objective function of threshold selection.

## 5. Conclusions

The inconsistent ways of flash drought definition, with one explicitly focusing on the intensification rate of soil moisture, and another considering its physical mechanism (e.g., PDFD and HWFD), are currently a major obstacle that hinders our understanding of this extreme

phenomenon. Following the conception of the intensification rate, in this study a new quantitative approach concerning the rate of soil moisture depletion during the onset-development phase is proposed, and its performance in terms of monitoring flash drought events, their onset time, and responses to the changes of vegetation are compared with those of PDFD and HWFD in the Yellow River basin. Overall, the rapid intensification-based approach can effectively track the sudden change of moisture status and is recommended for use. Since the approach of PDFD and HWFD neglects the change of soil moisture with time, it cannot ensure that the identified flash droughts all have the rapid evolving characteristic. In addition, the unreasonable thresholds associated with PDFD and HWFD limit their ability to capture the spatiotemporally continuous variation of drought. An investigation of the related meteorological variables suggests that the overly rigid temperature threshold is responsible for the poor behavior of PDFD and HWFD. Given the synchronous variation with soil moisture, PET could be viewed as a driver in the changes of soil moisture leading to flash droughts. Considering our research is based on a case study, evaluation of these flash drought identification methods for different regions and events is further needed. Findings from this study improve our understanding of flash drought, which also have some implications for promoting drought early warning techniques.

**Acknowledgments.** This work was supported by the National Key Research and Development Program approved by the Ministry of Science and Technology (Grant 2016YFA0601504), the National Natural Science Foundation of China (Grants 41807165, 41901037, 41701022, 51779070, 51579066), the National Natural Science Foundation of Jiangsu Province, China (Grant BK20180512), the Fundamental Research Funds for the Central Universities (2019B05214), the Natural Science Foundation of the Jiangsu Higher Education Institutions of China (19KJB170023), and the Belt and Road Special Foundation of the State Key Laboratory of Hydrology-Water Resources and Hydraulic Engineering (2018nkms05).

#### REFERENCES

- AghaKouchak, A., A. Farahmand, F. S. Melton, J. Teixeira, M. C. Anderson, B. D. Wardlow, and C. R. Hain, 2015: Remote sensing of drought: Progress, challenges and opportunities. *Rev. Geophys.*, **53**, 452–480, <https://doi.org/10.1002/2014RG000456>.
- Anderson, M. C., J. M. Norman, J. R. Mecikalski, J. A. Otkin, and W. P. Kustas, 2007: A climatological study of evapotranspiration and moisture stress across the continental United States based on thermal remote sensing. 2: Surface moisture climatology. *J. Geophys. Res.*, **112**, D11112, <https://doi.org/10.1029/2006JD007507>.
- Dorigo, W., and Coauthors, 2017: ESA CCI soil moisture for improved earth system understanding: State-of-the art and future directions. *Remote Sens. Environ.*, **203**, 185–215, <https://doi.org/10.1016/j.rse.2017.07.001>.
- Ford, T. W., and C. F. Labosier, 2017: Meteorological conditions associated with the onset of flash drought in the eastern United States. *Agric. For. Meteorol.*, **247**, 414–423, <https://doi.org/10.1016/j.agrformet.2017.08.031>.
- , and S. M. Quiring, 2019: Comparison of contemporary in situ, model, and satellite remote sensing soil moisture with a focus on drought monitoring. *Water Resour. Res.*, **55**, 1565–1582, <https://doi.org/10.1029/2018WR024039>.
- , D. B. McRoberts, S. M. Quiring, and R. E. Hall, 2015: On the utility of in situ soil moisture observations for flash drought early warning in Oklahoma, USA. *Geophys. Res. Lett.*, **42**, 9790–9798, <https://doi.org/10.1002/2015GL066600>.
- Hobbins, M. T., A. Wood, D. McEvoy, J. Huntington, C. Morton, M. C. Anderson, and C. Hain, 2016: The evaporative demand drought index: Part I: Linking drought evolution to variations in evaporative demand. *J. Hydrometeorol.*, **17**, 1745–1761, <https://doi.org/10.1175/JHM-D-15-0121.1>.
- Hoerling, M., J. Eischeid, A. Kumar, R. Leung, A. Mariotti, K. Mo, S. Schubert, and R. Seager, 2014: Causes and predictability of the 2012 great plains drought. *Bull. Amer. Meteor. Soc.*, **95**, 269–282, <https://doi.org/10.1175/BAMS-D-13-00055.1>.
- Hunt, E. D., K. G. Hubbard, D. A. Wilhite, T. Arkebauer, and A. L. Dutcher, 2009: The development and evaluation of a soil moisture index. *Int. J. Climatol.*, **29**, 747–759, <https://doi.org/10.1002/joc.1749>.
- , M. Svoboda, B. Wardlow, K. Hubbard, M. J. Hayes, and T. Arkebauer, 2014: Monitoring the effects of rapid onset of drought on non-irrigated maize with agronomic data and climate-based drought indices. *Agric. For. Meteorol.*, **191**, 1–11, <https://doi.org/10.1016/j.agrformet.2014.02.001>.
- Koster, R. D., S. D. Schubert, H. Wang, S. P. Mahanama, and A. M. DeAngelis, 2019: Flash drought as captured by reanalysis data: Disentangling the contributions of precipitation deficit and excess evapotranspiration. *J. Hydrometeorol.*, **20**, 1241–1258, <https://doi.org/10.1175/JHM-D-18-0242.1>.
- Liang, X., E. F. Wood, and D. P. Lettenmaier, 1996: Surface soil moisture parameterization of the VIC-2L model: Evaluation and modification. *Global Planet. Change*, **13**, 195–206, [https://doi.org/10.1016/0921-8181\(95\)00046-1](https://doi.org/10.1016/0921-8181(95)00046-1).
- Liu, Y., L. Ren, Y. Hong, Y. Zhu, X. Yang, F. Yuan, and S. Jiang, 2016: Sensitivity analysis of standardization procedures in drought indices to varied input data selections. *J. Hydrol.*, **538**, 817–830, <https://doi.org/10.1016/j.jhydrol.2016.04.073>.
- , Y. Zhu, L. Ren, V. P. Singh, X. Yang, and F. Yuan, 2017: A multiscalar Palmer drought severity index. *Geophys. Res. Lett.*, **44**, 6850–6858, <https://doi.org/10.1002/2017GL073871>.
- , —, —, B. Yong, S. Jiang, F. Yuan, and X. Yang, 2019: Understanding the spatiotemporal links between meteorological and hydrological droughts from a three-dimensional perspective. *J. Geophys. Res. Atmos.*, **124**, 3090–3109, <https://doi.org/10.1029/2018JD028947>.
- , —, L. Zhang, L. Ren, F. Yuan, X. Yang, and S. Jiang, 2020: Flash droughts characterization over China: From a perspective of the rapid intensification rate. *Sci. Total Environ.*, **704**, 135373, <https://doi.org/10.1016/J.SCITOTENV.2019.135373>.

- Mo, K. C., and D. P. Lettenmaier, 2015: Heat wave flash droughts in decline. *Geophys. Res. Lett.*, **42**, 2823–2829, <https://doi.org/10.1002/2015GL064018>.
- , and —, 2016: Precipitation deficit flash droughts over the United States. *J. Hydrometeor.*, **17**, 1169–1184, <https://doi.org/10.1175/JHM-D-15-0158.1>.
- Mozny, M., M. Trnka, Z. Zalud, P. Hlavinka, J. Nekovar, V. Potop, and M. Virag, 2012: Use of a soil moisture network for drought monitoring in the Czech Republic. *Theor. Appl. Climatol.*, **107**, 99–111, <https://doi.org/10.1007/s00704-011-0460-6>.
- Otkin, J. A., M. C. Anderson, C. Hain, I. E. Mladenova, J. B. Basara, and M. Svoboda, 2013: Examining rapid onset drought development using the thermal infrared based evaporative stress index. *J. Hydrometeor.*, **14**, 1057–1074, <https://doi.org/10.1175/JHM-D-12-0144.1>.
- , M. Shafer, M. Svoboda, B. Wardlow, M. C. Anderson, C. Hain, and J. Basara, 2015: Facilitating the use of drought early warning information through interactions with agricultural stakeholders. *Bull. Amer. Meteor. Soc.*, **96**, 1073–1078, <https://doi.org/10.1175/BAMS-D-14-00219.1>.
- , M. Svoboda, E. D. Hunt, T. W. Ford, M. C. Anderson, C. Hain, and J. B. Basara, 2018: Flash droughts: A review and assessment of the challenges imposed by rapid onset droughts in the United States. *Bull. Amer. Meteor. Soc.*, **99**, 911–919, <https://doi.org/10.1175/BAMS-D-17-0149.1>.
- Peng, J., A. Loew, O. Merlin, and N. E. C. Verhoest, 2017: A review of spatial downscaling of satellite remotely sensed soil moisture. *Rev. Geophys.*, **55**, 341–366, <https://doi.org/10.1002/2016RG000543>.
- Shukla, S., M. Safeeq, A. AghaKouchak, K. Guan, and C. Funk, 2015: Temperature impacts on the water year 2014 drought in California. *Geophys. Res. Lett.*, **42**, 4384–4393, <https://doi.org/10.1002/2015GL063666>.
- Trenberth, K. E., A. Dai, G. van der Schrier, P. D. Jones, J. Barichivich, K. R. Briffa, and J. Sheffield, 2014: Global warming and changes in drought. *Nat. Climate Change*, **4**, 17–22, <https://doi.org/10.1038/nclimate2067>.
- Wang, L., and X. Yuan, 2018: Two types of flash drought and their connections with seasonal drought. *Adv. Atmos. Sci.*, **35**, 1478–1490, <https://doi.org/10.1007/s00376-018-8047-0>.
- , —, Z. Xie, P. Wu, and Y. Li, 2016: Increasing flash droughts over China during the recent global warming hiatus. *Sci. Rep.*, **6**, 30571, <https://doi.org/10.1038/srep30571>.
- Wang, Z., R. Zhong, C. Lai, Z. Zeng, Y. Lian, and X. Bai, 2018: Climate change enhances the severity and variability of drought in the Pearl River Basin in South China in the 21st century. *Agric. For. Meteorol.*, **249**, 149–162, <https://doi.org/10.1016/j.agrformet.2017.12.077>.
- Yuan, X., Z. Ma, M. Pan, and C. Shi, 2015: Microwave remote sensing of short-term droughts during crop growing seasons. *Geophys. Res. Lett.*, **42**, 4394–4401, <https://doi.org/10.1002/2015GL064125>.
- , L. Wang, and E. F. Wood, 2018: Anthropogenic intensification of southern African flash droughts as exemplified by the 2015/16 season. *Bull. Amer. Meteor. Soc.*, **99**, S86–S90, <https://doi.org/10.1175/BAMS-D-17-0077.1>.
- Zhang, B., A. AghaKouchak, Y. Yang, J. Wei, and G. Wang, 2019: A water-energy balance approach for multi-category drought assessment across globally diverse hydrological basins. *Agric. For. Meteorol.*, **264**, 247–265, <https://doi.org/10.1016/j.agrformet.2018.10.010>.
- Zhang, Y., Q. You, C. Chen, and X. Li, 2017: Flash droughts in a typical humid and subtropical basin: A case study in the Gan River Basin, China. *J. Hydrol.*, **551**, 162–176, <https://doi.org/10.1016/j.jhydrol.2017.05.044>.